

Article

# External Radiation Assistance of Neutrinoless Double Electron Capture

Vladimir N. Kondratyev <sup>1,\*</sup>  and Feodor F. Karpeshin <sup>2</sup> <sup>1</sup> Bogolubov Laboratory of Theoretical Physics, JINR, 141980-RU Dubna, Russia<sup>2</sup> D.I. Mendeleev Institute for Metrology, 190005-RU Saint-Petersburg, Russia; fkarpeshin@gmail.com

\* Correspondence: vkondrat@jinr.ru

**Abstract:** The influence of electromagnetic radiation on nuclear processes is applied to an example of a neutrinoless double electron capture ( $0\nu 2ec$ ). For cases with X-ray free-electron lasers (X-ray FELs) and/or inverse Compton X-ray sources, it was shown that such a decay can be significantly enhanced by tuning the system to the resonant conditions through the absorption and/or emission of a photon with the decay resonance defect energy  $\Delta$ . In this case, the  $0\nu 2ec$  decay rate  $\Gamma_{2e}$  of nuclide  $Z$  grew linearly with field intensity ( $S/S_Z$ ) up to the X-ray flux power  $S_m \sim Z^6$ , while  $S_Z \sim Z^6 (\Gamma/\Delta)^2$  with decay width  $\Gamma$  of a daughter atom. For the case of  $^{78}\text{Kr} \rightarrow ^{78}\text{Se} - 0\nu 2eL_1L_1$  capture we find  $S_Z \sim 10^9 \text{ W cm}^{-2}$  and  $S_m \sim 10^{17} \text{ W cm}^{-2}$  which indicate a possibility of increasing decay rate to eight orders of magnitude or even larger.

**Keywords:** standard model; neutrinoless double electron capture; X-ray sources

## 1. Introduction

The evidence for physics beyond the Standard Model (SM) includes recent discoveries such as neutrino oscillations, adiabatic lepton flavor transformations and neutrino masses [1–5]. The direct hard probe for the lepton number violation and the Majorana nature of neutrinos [6] is provided by the neutrinoless double-beta ( $0\nu 2\beta$ ) decay [7] and/or double electron capture ( $0\nu 2ec$ ) processes that are forbidden within the SM. The breaking of global SM laws is illustrated by such phenomena that compel searches for experimental evidence and theoretical outlines of these effects. The double-beta ( $2\beta$ ) decay represents an isobaric transition from a parent nucleus ( $A, Z$ ) to a daughter nucleus ( $A, Z + 2$ ), adding two charges. In the two-neutrino, double-beta ( $2\nu 2\beta$ ) decay mode,  $(A, Z) \rightarrow (A, Z + 2) + 2 e^- + 2 \nu_e + Q_{\beta\beta}$ , with the energy released represented by the  $Q$ -value  $Q_{\beta\beta}$ . These SM-allowed, second-order weak decays correspond to a typical half-life of  $>10^{19}$  years.

The SM-forbidden  $0\nu 2\beta$  decay  $(A, Z) \rightarrow (A, Z + 2)^{++} + e^- + e^-$ , with a doubly ionized atom  $(A, Z + 2)^{++}$  in the final state, was first considered by Furry [8]. In this process of  $0\nu 2\beta$  decay, the nucleus with mass number  $A$  and charge  $Z$  is accompanied by the Majorana neutrino exchange between the nucleons (see Figure 1a in which  $Z$  changes by  $Z + 2$  and  $Z - 2$  changes by  $Z$ ). There are many models beyond the SM that provide alternative mechanisms of the  $0\nu 2\beta$  decay, e.g., [9,10] and refs. therein.

Winter suggested [11] a related  $0\nu 2ec$  process,  $e_b^- + e_b^- + (A, Z) \rightarrow (A, Z - 2)^{**}$ , with bound electrons  $e_b^-$ , excited states of the daughter nucleus and the electron shells of the neutral atom  $(A, Z - 2)^{**}$ . An example of a mechanism related to the Majorana neutrino exchange is shown in Figure 1a. Subsequent de-excitation of the daughter nucleus  $(A, Z - 2)^{**}$  proceeds via the Auger electron and/or gamma ray emission cascades with filling electronic shell vacancies.

The  $0\nu 2ec$  process is several orders of magnitude less sensitive to the Majorana neutrino mass than the  $0\nu 2\beta$  decay. Winter pointed out [12] that the energy degeneracy of parent  $(A, Z)$  and excited daughter  $(A, Z - 2)^{**}$  atoms gives rise to resonant enhancement



**Citation:** Kondratyev, V.N.; Karpeshin, F.F. External Radiation Assistance of Neutrinoless Double Electron Capture. *Atoms* **2024**, *12*, 27. <https://doi.org/10.3390/atoms12050027>

Academic Editor: Maxime Brodeur

Received: 3 February 2024

Revised: 19 April 2024

Accepted: 24 April 2024

Published: 28 April 2024



**Copyright:** © 2024 by the authors. Licensee MDPI, Basel, Switzerland. This article is an open access article distributed under the terms and conditions of the Creative Commons Attribution (CC BY) license (<https://creativecommons.org/licenses/by/4.0/>).

of the decay. Although such a possibility of resonant behavior was confirmed by numerous studies of the  $0\nu 2\text{ec}$  process, e.g., [13,14], the resonance-like coincidence in  $2\text{ec}$  is considered, as a doubtful option. Given the decay resonance defect  $\Delta = M_{A,Z} - M_{A,Z-2}^{**}$ , the difference in mass between the parent and daughter atoms in the decay probability is determined by the Breit–Wigner factor (see Section 2.1).

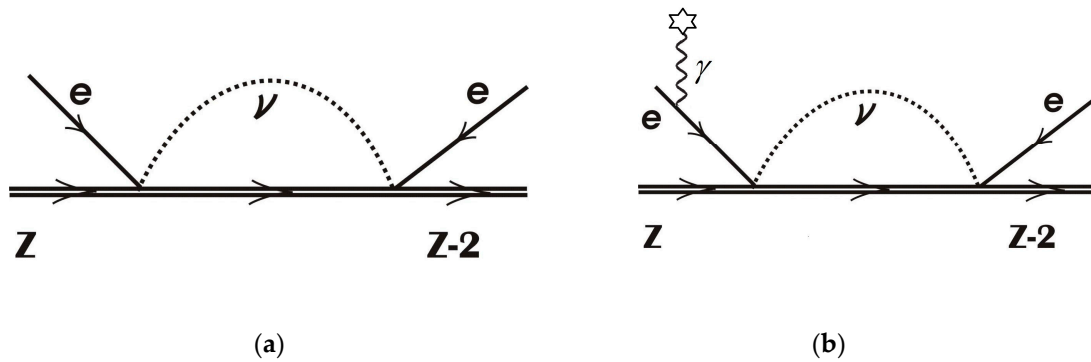


**Figure 1.** Schematic representation of neutrinoless double electron capture (a) for an isolated nuclide and (b) under the influence of X-ray flux.

The near-resonant  $0\nu 2\text{ec}$  process was analyzed in detail in ref. [15]. The authors developed a non-relativistic formalism of the resonant  $0\nu 2\text{ec}$  in atoms and specified a dozen nuclide pairs for which degeneracy is not excluded. Detailed theoretical predictions for a list of near-resonant  $0\nu 2\text{ec}$  nuclide pairs are provided in refs. [16–18]. Evidently, the proper fit of the difference between the masses of the parent and daughter atoms, i.e., Q-values, and the transition energy can result in a significant enhancement of the decay rate. Possibilities for an additional tuning of the degeneracy parameter  $\Delta$  have fundamental importance.

The manipulation of nuclear processes using irradiation from powerful X-ray sources, e.g., inverse Compton scattering X-ray sources [19,20], X-ray free-electron lasers (FELs) [21–23] and/or others [24], represents an extremely intriguing task of modern physics. For the purposes of these applications, the respective solutions can be used to trigger the release of enormous amounts of energy contained in nuclear isomers. In terms of fundamental research, this task is also of principal interest. The implementation of such a method is possible only through the involvement of the electronic shell, since the field of the strongest lasers is much smaller than the Coulomb field of the nucleus near its surface. The investigation of this fundamental process is of great interest from the point of view of understanding the nature of neutrinos. The discovery of a phenomenon such as  $0\nu 2\text{ec}$  would unambiguously indicate the Majorana nature of neutrinos (e.g., [9–18]). However, these investigations encounter great difficulties due to the very long lifetimes of the samples, so it would be difficult to overestimate the possibility of radically accelerating this process by several orders of magnitude.

This work aims to analyse potential tools to adjust the decay resonance defect  $\Delta$  to the correct zero value by applying an external field. In particular, we consider the effect of strong X-ray pulses that are relevant for inverse Compton scattering X-ray sources [19,20], X-ray FELs [21–23] and/or others [24].

## 2. Environmental Effect of the Neutrinoless Double Electron Capture ( $0\nu 2\text{ec}$ ) Process

Figure 1b represents a schematic diagram of the neutrinoless double electron capture ( $0\nu 2\text{ec}$ ) decay, which accounts for coupling to external radiation or the environment. Such an electromagnetic interaction is shown by the line  $\gamma$ , indicating a real or virtual photon. Hereafter, we consider external X-ray radiation.

### 2.1. Resonant Character of the Neutrinoless Double Electron Capture (0ν2ec)

In the case of 0ν2e capture, the atom remains generally neutral. Therefore, the energy release is determined by the difference in the masses of neutral atoms, the initial  $M_1$  and the daughter  $M_2$ , including its excitation energy  $E_A$ , as given by

$$Q = M_1 - M_2 - E_A. \tag{1}$$

Let us recall the formula for the traditional resonant fluorescent mechanism corresponding to the pole approximation. The capture of 0ν2ec leads to the formation of a doorway state. Due to the absence of degeneracy, it is located outside the mass surface, since its energy differs from the value  $E_A$  by the magnitude of the resonance defect  $\Delta = Q$ . Due to the uncertainty principle, a violation of the law of conservation of energy is possible for a time  $\tau = 1/Q$ ; hereafter, we use units with  $\hbar = 1$  to indicate otherwise. Then, a fluorescent or Auger transition occurs, resulting in a return of the atom to the mass surface. The energy of  $\Delta$  is added to the usual energy of this transition. This whole sequence of transformations forms a single, fast process. Formally, it is described by multiplying the square of the amplitude of the capture itself,  $\Gamma_{2e}$ , by the Breit–Wigner resonance factor  $B_W$ :

$$\Gamma_{2e}^i = \Gamma_{2e} B_W, \quad B_W = \frac{\Gamma/2\pi}{\Delta^2 + \Gamma^2/4}. \tag{2}$$

In Equation (2),  $\Gamma$  denotes the sum of the widths of the doorway state of a daughter atom with two holes before and after its decay. As seen in Table 1, for typical cases, the value  $\Delta$  varies from a few keV to hundreds keV, while the Breit–Wigner factor drops six or seven orders of magnitude. Here we draw attention to the way in which we can compensate the decay resonance defect  $\Delta$ .

$$\Gamma_{2e} = 2\pi |F_{2e}|^2, \quad F_{2e} = \langle \psi_2 | H'_{2e} | \psi_1 \rangle. \tag{3}$$

**Table 1.** Experimental data for nuclides associated with 0ν2ec decay. The resonance defect  $\Delta$  and the de-excitation width of the daughter nuclide electron shells  $\Gamma$  are relevant for the possible resonant enhancement value  $\Delta/\Gamma$ .

Transition [Ref.]	$\Delta$ (keV)	$\Gamma$ (eV)	$\Delta/\Gamma \cdot 10^3$
$^{36}\text{Ar} \rightarrow ^{36}\text{S}$ [25]	427.65	1.04	411.2
$^{40}\text{Ca} \rightarrow ^{40}\text{Ar}$ [26]	187.10	1.32	141.74
$^{50}\text{Cr} \rightarrow ^{50}\text{Ti}$ [27]	1159.7	1.78	651.5
$^{78}\text{Kr} \rightarrow ^{78}\text{Se}$ [28,29]	5.83	7.6	0.773
$^{196}\text{Hg} \rightarrow ^{196}\text{Pt}$ [30]	$661.8 \pm 3.0$	99	6.7
	$37.6 \pm 3.0$	58.3	0.645
$^{132}\text{Ba} \rightarrow ^{132}\text{Xe}$ [31]	774.8	23.0	33.7
$^{54}\text{Fe} \rightarrow ^{54}\text{Cr}$ [27]	668.3	2.04	327.6

Here,  $H'_{2e}$  and  $F_{2e}$  are the Hamiltonian and matrix elements of the double electron capture.

### 2.2. Resonance Tuning Using X-ray Radiation

The method of compensation of the resonance defect in the field of an intense electromagnetic wave was proposed in ref. [32] and described in detail in refs. [33,34]. Such a tool is completely general and can be applied in cases of both positive and negative values of  $\Delta$ . The excess energy of the decay can be transferred to the external field, while the missing energy can be drawn from the radiation. Such a method is particularly effective in the presence of an electric dipole junction in the system, preferably close to resonance.

In more detail, we consider the example of 0ν2eL<sub>1</sub>L<sub>1</sub> capture in  $^{78}\text{Kr}$  at the 2<sup>+</sup> 2838.49 keV level  $^{78}\text{Se}$  (see Table 1). In an experiment by Gavriluk et al. [28], which gives an example of the calorimetric approach, an indication of the 2ν2eK capture in  $^{78}\text{Kr}$  was obtained

with a proportional chamber filled with enriched  $^{78}\text{Kr}$ . This result was confirmed recently [29] with better statistical accuracy in a study that showed that the half-life of  $T_{1/2}^{2\nu 2K} = 1.9_{0.7}^{1.3}(\text{stat}) \pm 0.3(\text{syst}) \times 10^{22}$  yr. A diagram of the atomic levels is shown in Figure 2. It is convenient to measure the energy using the value for the selenium atom, assuming that the capture occurs in the ground state of the atomic shell according to Equation (1) (see Figure 2). In this case, we obtain  $Q = 9.15$  keV. Two remaining  $L_1$  holes, according to Figure 2, reduce this value by 3.32 keV to  $Q_{\text{eff}} = 5.84$  keV. Therefore, the resonance defect  $\Delta = Q_{\text{eff}} = 5.84$  keV (see Table 1). The state  $2p_{3/2}$  in the wave field acquires satellites in the wave function equidistant from the main level by an amount  $\pm n\omega_l$ ,  $n = 1, 2, 3, \dots$ , and the amplitudes decrease with the growth of  $n$ . For our purpose, the component with  $n = 1$  is essential. In this approximation, the  $L_1$  level forms two satellites,  $L_1^{(+)}$  and  $L_1^{(-)}$ , with the  $L_3$  state, with energies  $E_{L_3} \pm \omega_l$ , respectively. Here,  $E_{L_3}$  denotes the energy of the  $L_3$  level or the  $2p_{3/2}$  state (Figure 2). At a photon energy of  $\omega_l = 6.06$  keV, it falls exactly into resonance with the ground level of the parent atom, as shown in Figure 2. Evidently, such experimental conditions solve the tuning problem, i.e., the Breit–Wigner factor turns into one, when integrated over energy. The gain reaches a unitary maximum. We estimate the required radiation power.

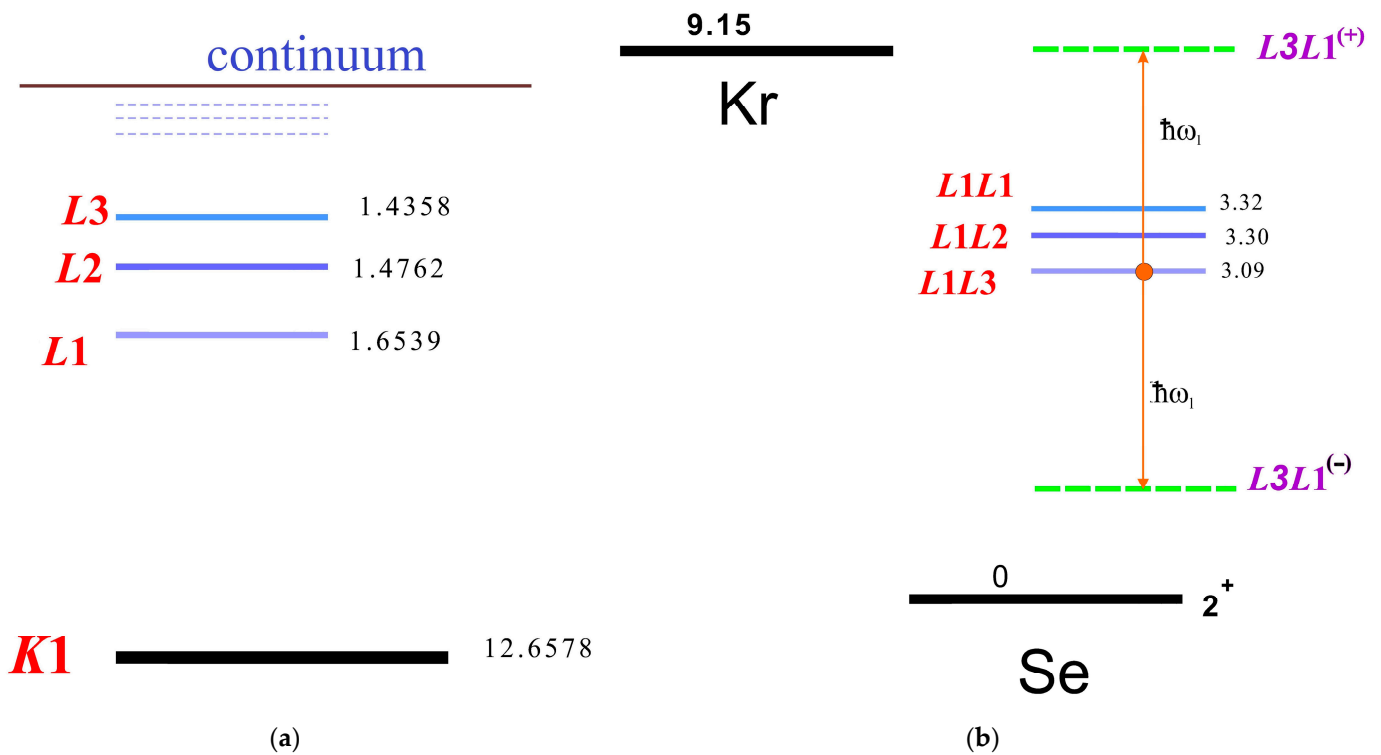


**Figure 2.** (a, left) Atomic level diagram of  $^{78}\text{Se}$  (in keV). (b, right) Compensation circuit for a resonance defect in the laser field. The energies of the two-hole states shown in the figure on the right are set equal to the sum of the energies of each of the holes shown in panel a. Energies are shown in keV.

The amplitude of the admixture of electronic states in a field reads

$$\beta = e\mathbf{E} \langle 2p | \mathbf{r} | 2s \rangle / \delta, \quad (4)$$

where  $\mathbf{E}$  denotes the intensity vector of the electric field of the laser,  $e$  is the charge of the electron,  $\mathbf{r}$  represents the spatial coordinate vector, and  $|2s\rangle$  and  $|2p\rangle$  indicate eigenfunctions for the 2s and 2p states, respectively. Here,  $\delta$  is equal to the difference between the energy of the additional component we need and the respective component itself.

Taking into account the admixture value in Equation (4), the wave function of the  $L_3$  electron in the exit channel (state after capture) can be written as

$$\psi_2 = (\psi_{L_3} + \beta \psi_{L_1} \exp\{-i\omega_l t\}) \exp\{-i E_{L_3}^h t\}, \quad (5)$$

where  $E_{L_3}^h$  is the energy of the  $L_3$  holes. It is worth noting here that this linear approximation for state mixing corresponds to the condition  $\beta < 1$ . These limits define the upper values of the electromagnetic field strength and the photon flux intensity power  $S_m$  for reliable implementation of the considered approach. Given that in a hydrogen-like model with nuclide effective charge  $Z$ , the dependence for  $\beta \sim Z^{-3}$ , and the photon flux power linear approximation limit  $S_m$  grows with  $Z$  as  $S_m \sim Z^6$ .

Substituting the full wave function into Equation (5), taking into account the time factor in Equation (3) and leaving only the component  $L_1$ , we obtain

$$F_{2e}^{(x)} = \langle \psi_2 | H'_{2e} | \psi_1 \rangle \exp\{-i (E_1 - E_2 - \omega_l) t\}. \quad (6)$$

The index 2 here is associated with the state  $\psi_{L_1}$ . Then, squaring the amplitude in Equation (3) in the usual way (e.g., [35]), we move on to consider the probability of the process per unit of time:

$$\Gamma_{2e}^x(\omega_l) = \beta^2 \Gamma_{2e} \frac{\Gamma/2\pi}{(E_1 - E_2 - \omega_l)^2 + \Gamma^2/4} \delta(E_1 - E_2 - \omega_l) \quad (7)$$

Taking into account Equation (7), we write the law of energy conservation in the form

$$M_1 = M_2 - E_{L_1} + E_{L_3} + \omega_r, \quad (8)$$

which provide conditions for the resonant frequency of the X-ray (laser) irradiation:

$$\omega_r = \Delta + E_{L_1} - E_{L_3}. \quad (9)$$

Thus, in the electromagnetic field, the capture of the second electron still occurs from the 2s subshell, but not just a hole is formed in its orbit: a hole mixed with the  $2p_{3/2}$  same hole state, with energy  $E_{L_3} + \omega_l$ , was formed. Under the condition given by Equation (9), this energy just resonates with the mass of the parent atom. Accordingly, from Equation (7), we obtain

$$\Gamma_{2e}^x = \Gamma_{2e} \frac{\Gamma/2\pi}{(\omega_l - \omega_r)^2 + \Gamma^2/4} S(\omega_l) d\omega_l, \quad (10)$$

where  $S(E)$  is the spectral density of the X-ray source or laser radiation. Integrating Equation (10) over the profile of the laser line, and assuming that the spectral width is close to  $\Gamma$  ( $S(E) \sim 1/\Gamma$ ), we write the decay rate in an electromagnetic field as

$$\Gamma_{2e}^x = \Gamma_{2e} \frac{\beta^2}{\Gamma}. \quad (11)$$

Incorporating the ratio in Equation (11) into Equation (2), we obtain a gain in the probability of this process in the X-ray radiation field in the following form:

$$G = \frac{\Gamma_{2e}^x}{\Gamma_{2e}} = 2\pi N \beta^2 \left(\frac{\Delta}{\Gamma}\right)^2 \quad (12)$$

where  $N = 8$  is determined by a statistical weight that takes into account the presence of two 2s holes and four  $2p_{3/2}$  electrons.

From the condition  $G \approx 1$ , we can estimate the value of  $\beta$  at which the probability of stimulated decay is compared with the natural one:  $\beta_x \approx 10^{-4}$ . Bearing in mind the parameters of the gamma factory at CERN [25] for estimation, we set the photon flux power with energy  $\omega_l = 5$  keV equal to  $4 \text{ MW cm}^{-2}$ . This power corresponds to a field strength of

60 kV/cm. The calculated value of the matrix element  $\langle 2p | \mathbf{r} | 2s \rangle \approx 22 \text{ keV}^{-1} \approx 4 \times 10^{-7} \text{ s}$ . From Figure 2 on the right (b), we find that  $\Delta \approx 5.84 \text{ keV}$ . Using Equation (4), we estimate the real admixture that occurs in such a field:  $\beta \approx 0.5 \times 10^{-5}$ . Thus, the entire order of intensity is missing, or three orders of magnitude in the power of the gamma ray flux of Swiss X-ray FELs.

### 3. Discussion

We analyse the effect of an intense electromagnetic field relevant for X-ray FELs, inverse Compton X-ray sources, etc., in the  $0\nu 2e c$  radioactive decay process. As was illustrated, the emission and/or absorption of X-ray photons can result in significant increases in the decay rate. Such strengthening of the beta-decay channel associated with the double electron capture process originates from tuning the resonance defect  $\Delta$  to zero and the system to the resonance conditions. A crucial requirement for an efficient photon absorption/emission is associated with a significant dipole coupling of substates in the electronic shell. The L-shell is well suited for this case. As was seen in Equations (4) and (5) and the discussion therein, the treatment of state mixing within perturbation theory is well justified up to an X-ray flux intensity of  $S_m \approx Z^6 \times 10^8 \text{ W cm}^{-2}$ . We employ here a hydrogen-like description of electronic states with an effective charge  $Z$ , which is rather reliable for the internal shells. In this range, the decay rate grows linearly with the electromagnetic field intensity  $G \approx S/S_z$  with  $S_z \approx Z^6 (\Gamma/\Delta)^2 \times 10^{5.5} \text{ W cm}^{-2}$ . At the upper limit of the application of perturbation theory with  $S_m$ , the enhancement factor is  $G_m \approx S_m/S_z \approx (\Delta/\Gamma)^2 \times 10^{2.5}$ . Such a feature shows that in the case of relatively weak X-ray flux power, the maximum factor for an increasing  $0\nu 2e c$  decay rate is determined by the ratio  $\Delta/\Gamma$  and amounts to about eight orders of magnitude.

To this end, let us estimate the rate of induced  $0\nu 2e L_1 L_1$  capture in  $^{78}\text{Kr}$  at the  $2^+$  2838.49 keV level  $^{78}\text{S}$  when the sample is irradiated by the X-ray flux with resonance frequency and an effective intensity  $S_{ef}$  close to the value  $S_m$ . The total number of decays per unit time is  $dN/dt \approx N_n \Gamma_{ef}$ , with the total number of atoms in a sample  $N_n$  and an effective X-ray assisted transition width  $\Gamma_{ef} = S_{ef} \Gamma_{2e} \approx \Gamma_{res} \approx 10^{-20} \text{ yr}^{-1}$ . For a case in which  $N_n \approx 10^{28.5}$ , i.e., 3 tons of the material (e.g., the Gran Sasso experiment), the decay rate rises to 10 per second. Alternatively, to enhance the effect, one can imagine an ampoule of liquid  $^{78}\text{Kr}$ , 1 m long with a  $1 \text{ cm}^2$  cross-section, positioned along the beam. In this case, the counting rate would be four orders of magnitude lower, which, however, is quite sufficient for experimental observations. Evidently, additional evidence for the considered events are provided by subsequent  $\Gamma$  decays of the daughter nucleus and radiative transitions due to relaxation of the L-shell holes. Such an accompanying emission of photons and Auger electrons is very favorable for detection and ensures a registration probability of tens percent.

It is worth noting that although the intensity electromagnetic field,  $S_m$ , considered here is much less than the upper power limit due to, e.g., the vacuum short circuit, the present intensities of gamma ray sources are still very small compared to the  $S_m$  value. However, very strong X-ray fluxes arise during astrophysical phenomena, e.g., supernova explosions, which have an important role in neutrino nuclear reactions [36].

### 4. Conclusions

In this study, we performed evaluations of the electromagnetic field effects for the possible acceleration of the neutrinoless double electron capture process. Unfortunately, the example discussed above suggests that the power of the gamma factory flow is not yet sufficient to radically manipulate this process. In conjunction with the present status of X-ray source intensities, we employed perturbation theory for the evaluation of the respective effects of the decay rate acceleration. As a result, we found that the decay rate grew linearly with increasing X-ray flux intensity up to ten orders of magnitude. Evidently, the design of X-ray fabrics such as X-ray FELs, inverse Compton X-ray sources, etc., has developed rapidly over the last two decades (see refs. [19–24]), which gives hope for a

reassessment of possibilities in the future. The results obtained above should be perceived as an assessment of the parameters necessary to achieve the goals stated in this work.

**Author Contributions:** Conceptualization, V.N.K. and F.F.K.; methodology, V.N.K. and F.F.K.; software, V.N.K. and F.F.K.; validation, V.N.K. and F.F.K.; formal analysis, V.N.K. and F.F.K.; investigation, V.N.K. and F.F.K.; data curation, V.N.K. and F.F.K.; writing—original draft preparation, V.N.K. and F.F.K.; writing—review and editing, V.N.K. and F.F.K.; visualization, V.N.K. and F.F.K.; supervision, F.F.K. All authors have read and agreed to the published version of the manuscript.

**Funding:** This research received no external funding.

**Data Availability Statement:** Available on a request.

**Acknowledgments:** The authors are grateful to D. Budker for useful discussions of the available experimental installations with intense sources of electromagnetic fields.

**Conflicts of Interest:** The authors declare no conflicts of interest.

## References

1. Fukuda, Y.; Hayakawa, T.; Ichihara, E.; Inoue, K.; Ishihara, K.; Ishino, H.; Itow, Y.; Kajita, T.; Kameda, J.; Kasuga, S.; et al. Evidence for Oscillation of Atmospheric Neutrinos. *Phys. Rev. Lett.* **1998**, *81*, 1562. [\[CrossRef\]](#)
2. Ahmad, Q.R.; Allen, R.C.; Andersen, T.C.; Anglin, J.D.; Barton, J.C.; Beier, E.W.; Bercovitch, M.; Bigu, J.; Biller, S.D.; Black, R.A.; et al. Direct Evidence for Neutrino Flavor Transformation from Neutral-Current Interactions in the Sudbury Neutrino Observatory. *Phys. Rev. Lett.* **2002**, *89*, 011301. [\[CrossRef\]](#)
3. Eguchi, K.; Enomoto, S.; Furuno, K.; Goldman, J.; Hanada, H.; Ikeda, H.; Ikeda, K.; Inoue, K.; Ishihara, K.; Itoh, W.; et al. First Results from KamLAND: Evidence for Reactor Antineutrino Disappearance. *Phys. Rev. Lett.* **2003**, *90*, 021802. [\[CrossRef\]](#) [\[PubMed\]](#)
4. Kajita, T. Nobel Lecture: Discovery of atmospheric neutrino oscillations. *Rev. Mod. Phys.* **2016**, *88*, 030501. [\[CrossRef\]](#)
5. McDonald, A.B. Nobel Lecture: The Sudbury Neutrino Observatory: Observation of flavor change for solar neutrinos \*. *Rev. Mod. Phys.* **2016**, *88*, 030502. [\[CrossRef\]](#)
6. Majorana, E. Teoria simmetrica dell'elettrone e del positrone. *Nuovo Cim.* **1937**, *14*, 171–184. [\[CrossRef\]](#)
7. Schechter, J.; Valle, J.W.F. Neutrinoless Double beta Decay in  $SU(2) \times U(1)$  Theories. *Phys. Rev. D* **1982**, *25*, 2951. [\[CrossRef\]](#)
8. Furry, W.H. On Transition Probabilities in Double Beta-Disintegration. *Phys. Rev.* **1939**, *56*, 1184–1193. [\[CrossRef\]](#)
9. Dolinski, M.J.; Poon, A.W.; Rodejohann, W. Neutrinoless double-beta decay: Status and prospects. *Annu. Rev. Nucl. Part. Sci.* **2019**, *69*, 219–251. [\[CrossRef\]](#)
10. Blaum, K.; Eliseev, S.; Danevich, F.A.; Tretyak, V.I.; Kovalenko, S.; Krivoruchenko, M.I.; Novikov, Y.N.; Suhonen, J. Neutrinoless double-electron capture. *Rev. Mod. Phys.* **2020**, *92*, 045007. [\[CrossRef\]](#)
11. Winter, R.G.; Double, K. Capture and Single K Capture with Positron Emission. *Phys. Rev.* **1955**, *100*, 142–144. [\[CrossRef\]](#)
12. Winter, R.G. Search for Double Beta Decay in Cadmium and Molybdenum. *Phys. Rev.* **1955**, *99*, 88. [\[CrossRef\]](#)
13. Georgi, H.M.; Glashow, S.L.; Nussinov, S. Unconventional model of neutrino masses. *Nucl. Phys. B* **1981**, *193*, 297–316. [\[CrossRef\]](#)
14. Voloshin, M.B.; Mitsel'makher, G.V.; Eramzhyan, R.A. Conversion of an atomic electron into a positron and double  $\beta +$  decay. *JETP Lett.* **1982**, *35*, 656–659.
15. Bernabeu, J.; De Rujula, A.; Jarlskog, C. Neutrinoless double electron capture as a tool to measure the electron neutrino mass. *Nucl. Phys. B* **1983**, *223*, 15–28. [\[CrossRef\]](#)
16. Sujkowski, Z.; Wycech, S. Neutrinoless double electron capture: A tool to search for Majorana neutrino. *Phys. Rev. C* **2004**, *70*, 052501. [\[CrossRef\]](#)
17. Karpeshin, F.F. On neutrinoless double e capture problem. *Phys. Part. Nucl. Lett.* **2008**, *5*, 379–382. [\[CrossRef\]](#)
18. Karpeshin, F.F.; Trzhaskovskaya, M.B. Shake-off in the  $^{164}\text{Er}$  neutrinoless double electronic capture and the dark matter puzzle. *Phys. Rev. C* **2023**, *107*, 045502. [\[CrossRef\]](#)
19. Brümmer, T.; Bohlen, S.; Grüner, F.; Osterhoff, J.; Pöder, K. Compact all-optical precision-tunable narrowband hard Compton X-ray source. *Sci. Rep.* **2022**, *12*, 16017. [\[CrossRef\]](#) [\[PubMed\]](#)
20. Zheng, X. Inverse Compton gamma-ray source driven by a plasma flying mirror. *JOSA B* **2023**, *4*, 3262–3268. [\[CrossRef\]](#)
21. Geloni, G.; Saldin, E.; Samoylova, L.; Schneidmiller, E.; Sinn, H.; Tschentscher, T.; Yurkov, M. Coherence properties of the European XFEL. *New J. Phys.* **2010**, *12*, 035021. [\[CrossRef\]](#)
22. Milne, C.J.; Schietinger, T.; Aiba, M.; Alarcon, A.; Alex, J.; Anghel, A.; Arsov, V.; Beard, C.; Beaud, P.; Bettoni, S.; et al. SwissFEL: The Swiss X-ray free electron laser. *Appl. Sci.* **2017**, *7*, 720. [\[CrossRef\]](#)
23. Duris, J.; Li, S.; Driver, T.; Champenois, E.G.; MacArthur, J.P.; Lutman, A.A.; Zhang, Z.; Rosenberger, P.; Aldrich, J.W.; Coffee, R.; et al. Tunable isolated attosecond X-ray pulses with gigawatt peak power from a free-electron laser. *Nat. Photonics* **2020**, *14*, 30–36. [\[CrossRef\]](#)

24. Budker, D.; Berengut, J.C.; Flambaum, V.V.; Gorchtein, M.; Jin, J.; Karbstein, F.; Krasny, M.W.; Litvinov, Y.A.; Pálffy, A.; Pascalutsa, V.; et al. Expanding Nuclear Physics Horizons with the Gamma Factory (Ann. Phys. 3/2022). *Ann. Phys.* **2022**, *534*, 2270005. [[CrossRef](#)]
25. Agostini, M.; GERDA Collaboration; Allardt, M.; Bakalyarov, A.M.; Balata, M.; Barabanov, I.; Barros, N.; Baudis, L.; Bauer, C.; Bellotti, E.; et al. Limit on the radiative neutrinoless double electron capture of  $^{36}\text{Ar}$  from GERDA Phase I. *Eur. Phys. J. C* **2016**, *76*, 652. [[CrossRef](#)]
26. Angloher, G.; Bauer, M.; Bauer, P.; Bavykina, I.; Bento, A.; Bucci, C.; Canonica, L.; Ciemniak, C.; Defay, X.; Deuter, G.; et al. New limits on double electron capture of  $^{40}\text{Ca}$  and  $^{180}\text{W}$ . *J. Phys. G* **2016**, *43*, 095202. [[CrossRef](#)]
27. Bikit, I.; Krmar, M.; Slivka, J.; Vesković, M.; Čonkić, L.; Aničin, I. New results on the double  $\beta$  decay of iron. *Phys. Rev. C* **1998**, *58*, 2566. [[CrossRef](#)]
28. Gavriluk, Y.M.; Gangapshev, A.M.; Kazalov, V.V.; Kuzminov, V.V.; Panasenko, S.I.; Ratkevich, S.S. Indications of  $2\nu 2K$  capture in  $^{78}\text{Kr}$ . *Phys. Rev. C* **2013**, *87*, 035501. [[CrossRef](#)]
29. Ratkevich, S.S.; Gangapshev, A.M.; Gavriluk, Y.M.; Karpeshin, F.F.; Kazalov, V.V.; Kuzminov, V.V.; Yakimenko, S.P. Comparative study of the double-K-shell-vacancy production in single-and double-electron-capture decay. *Phys. Rev. C* **2017**, *96*, 065502. [[CrossRef](#)]
30. Bukhner, E.; Vishnevskij, I.N.; Danevich, F.A. Rare decays of mercury nuclei. *Sov. J. Nucl. Phys.* **1990**, *52*, 193–197.
31. Meshik, A.P.; Hohenberg, C.M.; Pravdivtseva, O.V.; Kapusta, Y.S. Weak decay of  $^{130}\text{Ba}$  and  $^{132}\text{Ba}$ : Geochemical measurements. *Phys. Rev. C* **2001**, *64*, 035205. [[CrossRef](#)]
32. Zon, B.A.; Karpeshin, F.F. Acceleration of the decay of  $^{235}\text{mU}$  by laser-induced resonant internal conversion. *Sov. Phys. JETP* **1990**, *70*, 224.
33. Karpeshin, F.F. *Instantaneous Fission in Muonic Atoms and Resonance Conversion*; Nauka: St. Petersburg, Russia, 2006. (In Russian)
34. Karpeshin, F.F. Resonance Internal Conversion as the way of accelerating nuclear processes. *Phys. Part. Nucl.* **2006**, *37*, 522. [[CrossRef](#)]
35. Landau, L.D.; Lifshitz, E.M. Quantum Mechanics: Non-Relativistic Theory. In *Course of Theoretical Physics*; Pergamon: New York, NY, USA, 1977; Volume 3.
36. Kondratyev, V.N. Magnetorotational supernova neutrino emission spectra and prospects for observations by large-size underwater telescopes. *Phys. At. Nucl.* **2023**, *86*, 1083–1089. [[CrossRef](#)]

**Disclaimer/Publisher's Note:** The statements, opinions and data contained in all publications are solely those of the individual author(s) and contributor(s) and not of MDPI and/or the editor(s). MDPI and/or the editor(s) disclaim responsibility for any injury to people or property resulting from any ideas, methods, instructions or products referred to in the content.